HNUE JOURNAL OF SCIENCE
Natural Sciences 2024, Volume 69, Issue 2, pp. 58-65
This paper is available online at http://hnuejs.edu.vn/ns
DOI: 10.18173/2354-1059.2024-0020

MOLECULAR DYNAMICS SIMULATION OF STRUCTURAL PROPERTIES OF Al_2O_3-SiO_2-CaO OXIDE DURING THE COOLING PROCESS

Le Van Vinh[1,2] and Nguyen Thi Thao[3,*]

[1]*Faculty of Computer Science, Phenikaa University, Hanoi city, Vietnam*
[2]*Phenikaa Research and Technology Institute (PRATI), A&A Green Phoenix Group, Hanoi city, Vietnam*
[3]*Faculty of Physics, Hanoi National University of Education, Hanoi city, Vietnam*

*Corresponding author: Nguyen Thi Thao, email: thaont@hnue.edu.vn

Received June 5, 2024. Revised June 21, 2024. Accepted June 28, 2024.

Abstract. The change of structural properties of Al_2O_3-SiO_2-CaO oxide during the cooling process was studied using the molecular dynamic simulation. The microstructures of the sample were investigated through the radial distribution function (RDF), coordination number (CN), and bond angle (BA) distribution. The results show a structural change from the liquid state to the amorphous state when the sample is cooled from 4000 K to 300 K. The glass transition occurs at T_g = 1585 K. The fraction of AlO_4, CaO_6, and SiO_4 units increases with decreasing temperature and dominates at 300 K.

Keywords: MD simulation, Al_2O_3-SiO_2-CaO oxide, cooling process, microstructures.

1. Introduction

The microstructural and thermodynamic properties of Al_2O_3-SiO_2-CaO oxides are important topics of both theoretical and experimental studies [1], [2]. Al_2O_3-SiO_2-CaO oxides are a significant component of magmas on Earth, where their thermodynamic properties strongly depend on their microstructural characteristics [3]. The structure of Al_2O_3-SiO_2-CaO oxides is a network structure with intermixed oxides SiO_2 and Al_2O_3 forming a tetrahedral network. The addition of Ca^{2+} cation into the SiO_4 and AlO_4 tetrahedral network leads to the formation of nonbridging oxygens (NBOs) alongside the bridging oxygens - BOs [4]. So Ca^{2+} cations play the role of network modifier. BO sites link AlO_4 or SiO_4 tetrahedral to form strong bonds, while NBO sites connect AlO_4 or SiO_4 tetrahedrons to Ca^{2+} to form relatively weak bonds. In the liquid state, Al_2O_3-SiO_2-CaO oxides have an Al-O network containing mostly AlO_4 units and a small fraction of AlO_3 and AlO_5 units. The Si-O network contains mostly SiO_4 units and a very small fraction of SiO_3 units. The Ca-O network contains CaO_4, CaO_5, CaO_6, CaO_7, and CaO_8 units, with

CaO_6 units being the main component. In the glass state, Al_2O_3-SiO_2-CaO oxides have a negligible fraction of AlO_3 and AlO_5 units, while the fraction of CaO_6 units increases significantly and no SiO_3 units are detected [4]-[7]. Atomic-level simulation studies have investigated the structural properties and phase transition of Al_2O_3-SiO_2-CaO oxide [8]-[9]. The simulation results of structural properties, such as the bond lengths of Al-O, Si-O, and Ca-O, the CN of O atoms around Al, Si, and Ca atoms are in good agreement with the experimental data. The simulation results of bond angle distribution showed that the O-Si-O bond angle distribution has a peak at 108.2°, which is close to the angle of a regular tetrahedron, 109.4°. Meanwhile, the O-Al-O BA distribution is wider than the O-Si-O angle distribution and has a peak at 107.2°. Thus, both experiments and simulations show that Al_2O_3-SiO_2-CaO oxide has an Al-O, Si-O, and Ca-O network structure with the main structural units being AlO_4, SiO_4, and CaO_6. In this study, we investigated the structural characteristics of Al_2O_3-SiO_2-CaO oxide during the cooling process using MD simulation. Structural analysis such as PRDF, CN, and bond angle distribution are used to clarify the phase transition from liquid to glass state.

2. Content

2.1. Computational method

MD simulation was used to construct Al_2O_3-SiO_2-CaO samples at different temperatures after the cooling process. In this study, to describe the interaction between atoms, we use the following potential function [10]:

$$U(r_{ij}) = \frac{z_i z_j e^2}{4\pi\varepsilon_0 r_{ij}} + A_{ij}\exp\left(-\frac{r_{ij}}{\rho_{ij}}\right) - \frac{C_{ij}}{r_{ij}^6}$$

This function includes two components: the long-range Coulomb force ($\frac{z_i z_j e^2}{4\pi\varepsilon_0 r_{ij}}$) and the short-range Buckingham potential function ($A_{ij}\exp\left(-\frac{r_{ij}}{\rho_{ij}}\right) - \frac{C_{ij}}{r_{ij}^6}$). The parameters of Buckingham potentials are shown in Table 1.

Table 1. The Buckingham potential parameters [10]

Pair	A_{ij} ***(eV)***	ρ_{ij} **(Å)**	C_{ij} **(eV•Å^6)**
Al-O	12201.417	0.195620	31.997
Si-O	13702.905	0.193810	54.681
Ca-O	7747.1834	0.252623	93.109
O-O	2029.2204	0.343640	192.58

Periodic boundary conditions are used to construct the simulation cubic box. The sample contains 10000 atoms with 6000 O atoms, 1000 Al atoms, 1500 Si atoms, and 1500 Ca atoms. First, the simulation box was heated at a temperature of 4000 K for 100 ps

and a pressure of 1 atm in NPT ensembles (constant pressure and temperature). Then, the sample was cooled from 4000 K to 300 K using the cooling rate of 4 K/ps. During the cooling process, the coordinates of atoms in the sample are saved at determined temperatures for structural analysis such as total RDF, PRDF, distribution of CN, and BA distribution.

2.2. Results and discussions

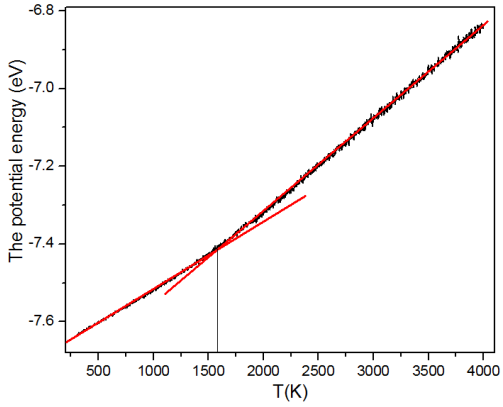

Figure 1. The potential energy of the sample during the cooling process

During the cooling process, we determined the average PE of atoms at the given temperatures. The evolution of the PE during the cooling process of the sample from 4000 K to 300 K is shown in Figure 1. When the temperature decreases, we observe a decrease in the value of PE. This result indicates that the system returns to a more stable state at a temperature of 300 K. To find the glass transition temperature, we determined the position where the slope of PE dependence on temperature changes between high and low-temperature regions. Accordingly, the T_g of Al_2O_3-SiO_2-CaO oxide is 1585 K. The glass transition temperature of this material sample, T_g=1585 K, is consistent with the experimental [6] and MD simulation data [8]. The structural change of the sample is shown by examining the change of both the total RDF and the pair RDF. Figure 2 depicts the total RDF of Al_2O_3-SiO_2-CaO oxide at different temperatures during the cooling process from 4000 K to 300 K.

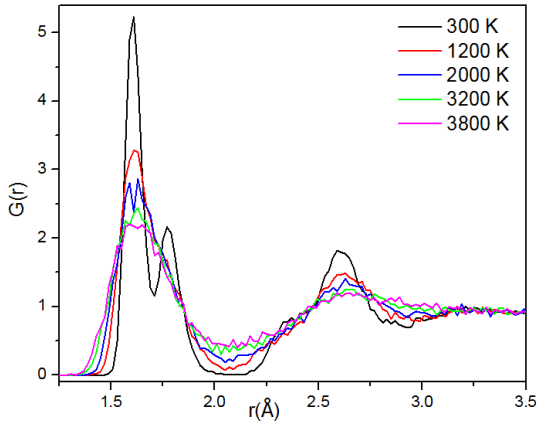

Figure 2. The total radial distribution function of the sample during the cooling process

The result in Figure 2 shows that at a high temperature of 3800 K, the total RDF curve has a high first peak with a fairly large width, and the second peak is lower and narrower. This indicates that the Al_2O_3-SiO_2-CaO oxide has a short-range order structure at 3800 K. As the temperature decreases, the height of the first peak of the total RDF increases and the width of the first peak narrows. It demonstrates that the sample becomes more ordered during the cooling process.

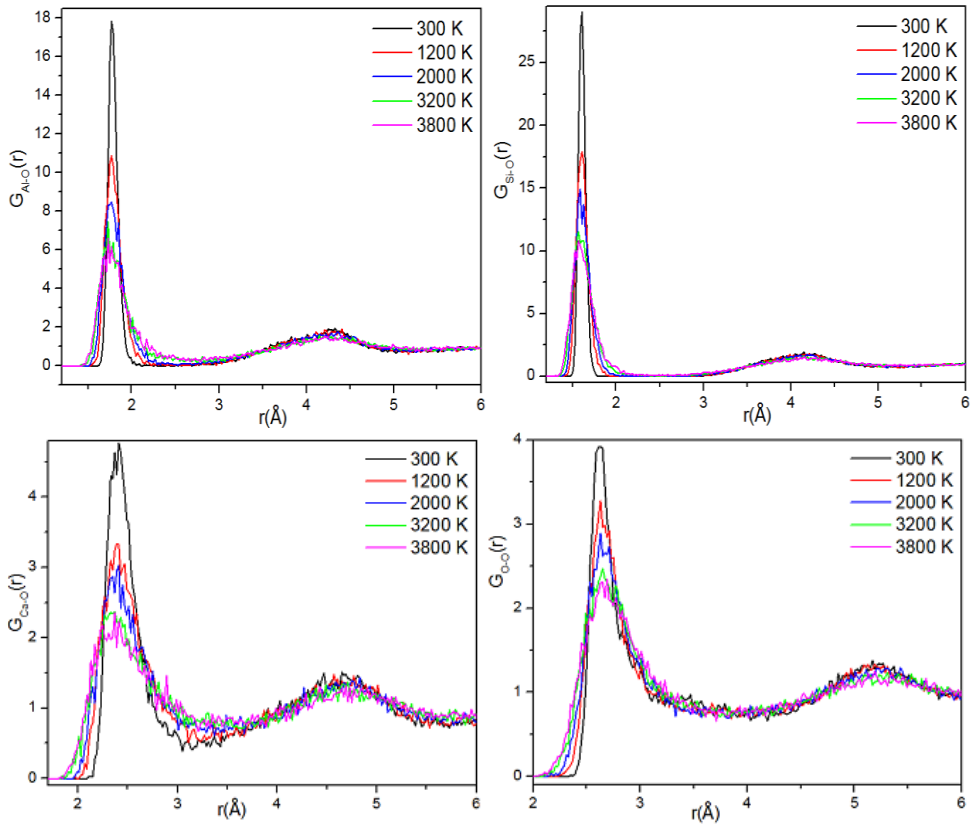

Figure 3. The pair radial distribution function (PRDF) of X-O (X: Al, Si, Ca, O) pair of the sample during the cooling process

Figure 3 depicts the PRDFs of Al-O, Si- O, Ca- O, and O-O pairs. The result shows that for all pairs, the first peak increases in height as temperature decreases. This indicates that the structure of the sample becomes more ordered as the temperature decreases. From the position of the first peak of the PRDF, we calculate the average bond length (BL) of atoms in the sample. For the Al-O pair, the position of the first peak increases from 1.71 Å at 3800 K to 1.77 Å at 300 K. Therefore, the average Al-O BL is a 1.71 Å and 1.77 Å at temperatures of 3800 K and 300 K, respectively. For the Si- O pair, the average Si - O BL is 1.61 Å and this value does not change with temperature. The average Ca -O BL is 2.27 Å at 3800 K and increases to the value of 2.39 Å at 300 K. In contrast to Al-O, Si-O and Ca- O, the position of the first peak of the PRDF for O- O pair decreases from 2.67 Å at 3800 K to 2.59 Å at 300 K. The Al-O, Si-O, and Ca-O BLs of sample are in good

agreement with experiment data: 1.76 ± 0.02 Å for Al-O, 1.62 ± 0.02 Å for Si-O and 2.35 ± 0.05 Å for Ca-O [6], [7].

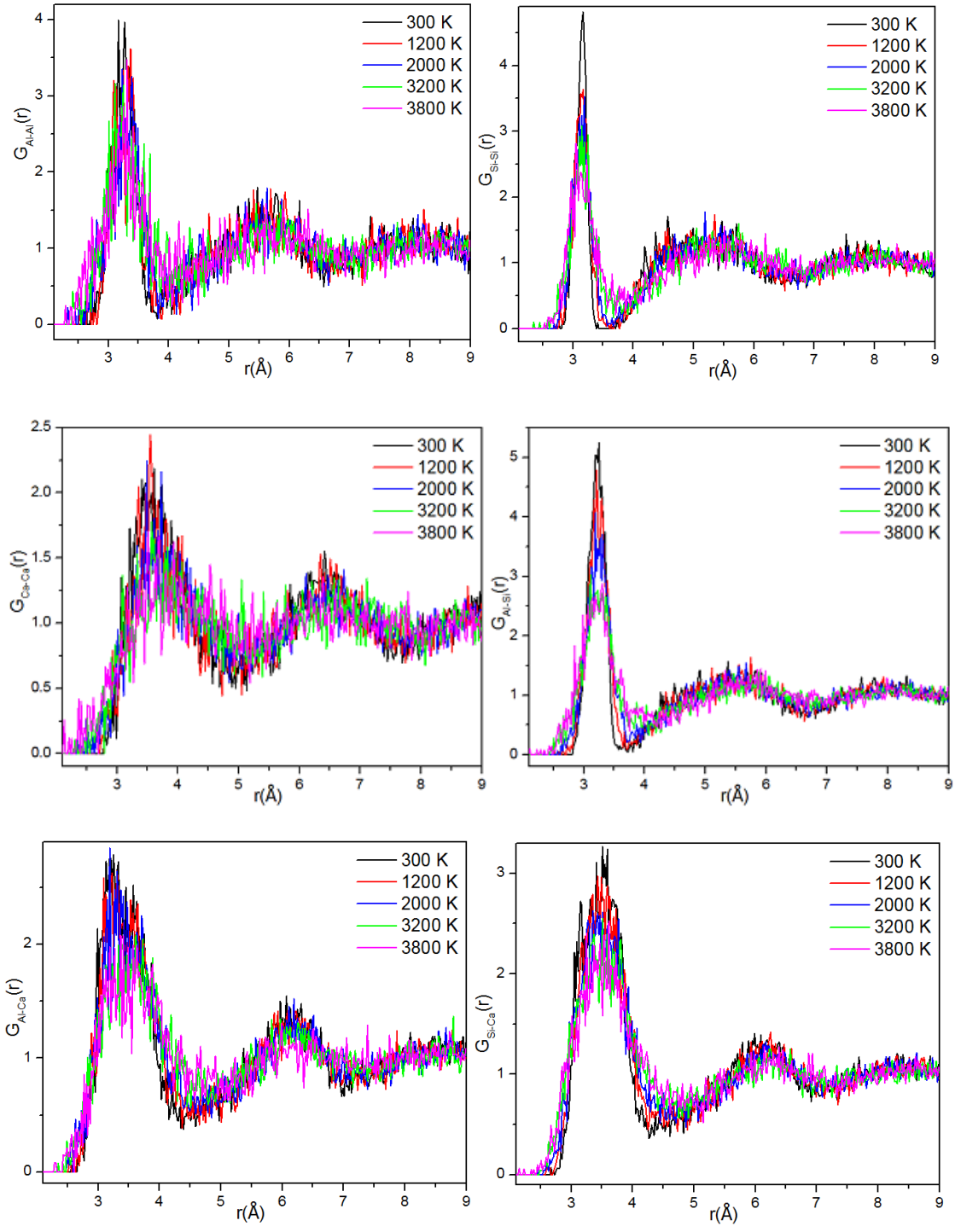

Figure 4. The pair radial distribution function (PRDF) of the X-Y (X, Y: Al, Si, Ca) pair of the sample during the cooling process

The PRDFs curves of the remaining pairs in the sample are shown in Figure 4. The PRDF curves have a strong disturbance at high temperatures indicating strong relative motion between two atoms. The atoms with the most displacement are Ca atoms and those with the least displacements are Si atoms. As the temperature decreases, the thermal motion of these atoms decreases. The distribution of several O coordination of Al, Si, and Ca atoms changes with the change in temperature as shown in Figure 5. For the CN distribution of Si atoms, most Si atoms have four neighboring O atoms forming SiO_4 tetrahedral at temperature low-temperature regions. At high temperatures, there is a small fraction of SiO_3 units. For Al-O CN distribution, at high temperatures, most Al atoms have four-fold and three-fold CN forming AlO_4 and AlO_3 units, respectively. As the temperature drops below 2000 K, the fraction of AlO_4 units gets the maximum value of 99.4 % at 300 K. The distribution of neighboring O atoms of Ca atoms is quite different from that of neighboring O atoms of Al and Si atoms. The number of neighboring O atoms of Ca atoms varies from 2 to 8 atoms. Fractions of CaO_4, CaO_5, CaO_6, and CaO_7 are 3.93 %, 26.93 %, 45.40 %, and 20.4 % respectively, at 300 K. The results for the number of coordination atoms of O around the Al, Si, and Ca atoms are consistent with previous research results [4]-[7].

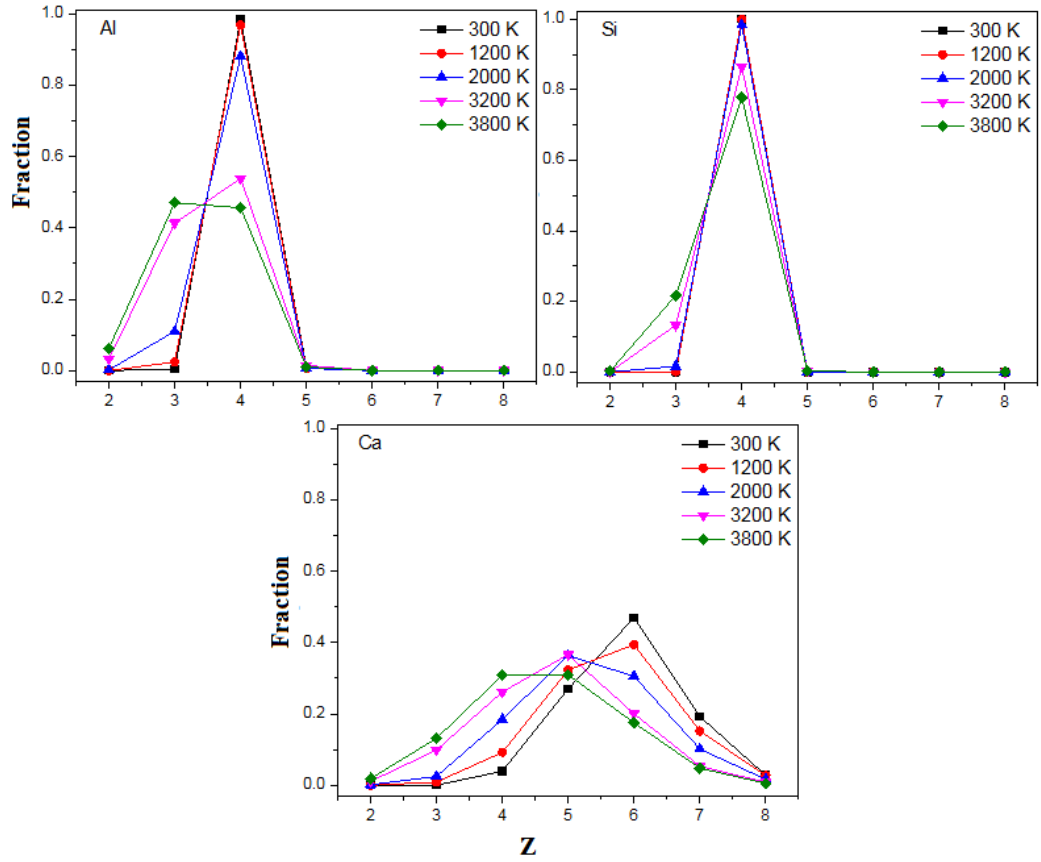

Figure 5. The distribution of coordination number of Al, Si, and Ca atoms at different temperatures

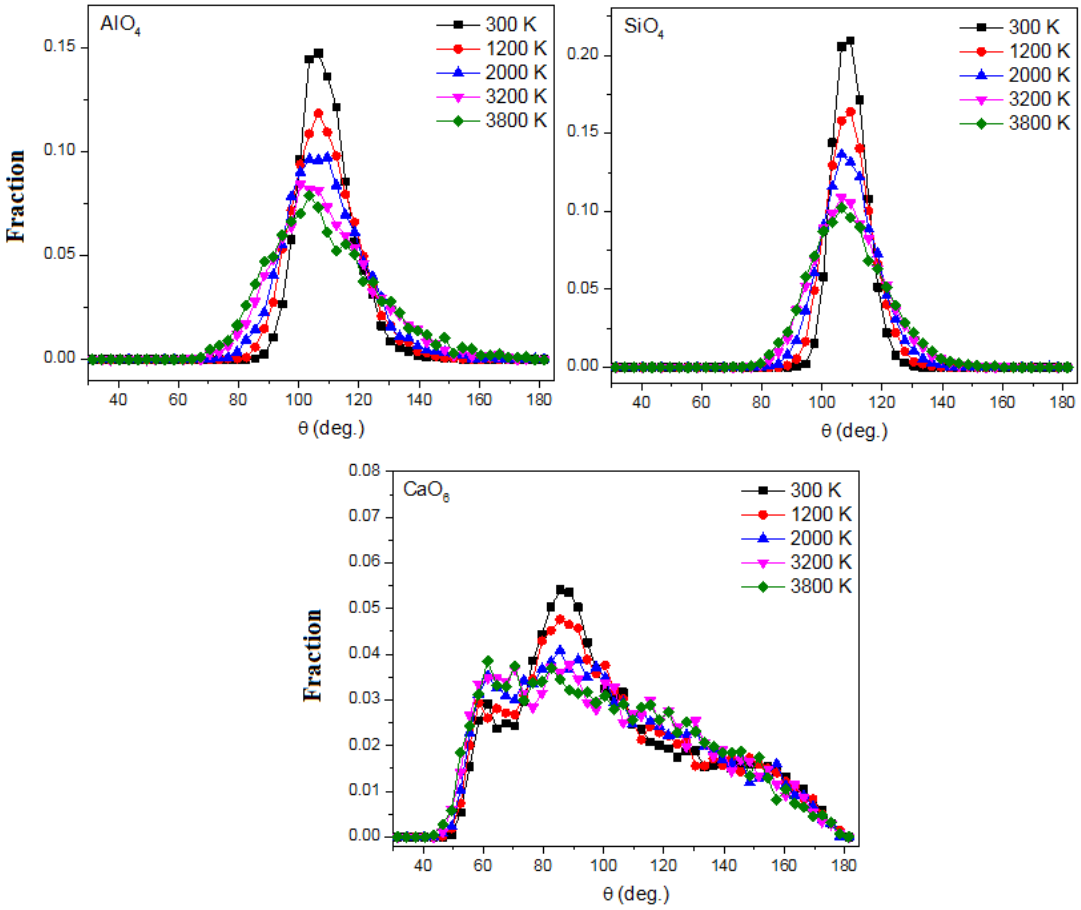

Figure 6. The distribution of O-Al-O, O-Si-O and O-Ca-O bond angles in AlO_4, SiO_4 and CaO_6 respectively, at different temperatures

To clarify the structural properties of the Al_2O_3-SiO_2-CaO oxide system, the O-Al-O, O-Si-O, and O-Ca-O BA distributions in AlO_4, SiO_4, and CaO_6 units respectively are calculated and shown in Fig.6. We observe that the distribution of O-Al-O BA is broad and has a peak at 109.5° at 3800 K and it has a peak at 106.5° at 300 K. This indicates that atoms have four neighboring O atoms forming AlO_4 regular tetrahedron at 300 K. The average O-Si-O BA is about 106.5° at 300 K, similar to the average O-Al-O BA. The distribution of O-Ca-O BA has a peak at 88.5° at 300 K. This means that the octahedron formed by 6 O atoms and Ca atoms tends to be a regular octahedron at 300 K.

3. Conclusions

The microstructural properties of Al_2O_3-SiO_2-CaO oxide were computed using molecular dynamics simulations. The structural analyses used include the RDF, PRDF, CN distribution, and BA distribution. The glass transition temperature was characterized by the change of potential energy during the cooling process and it occurs at T_g =1585 K. The fraction of AlO_4, CaO_6, and SiO_4 units increases with the decreasing of temperature and dominates at a temperature of 300 K.

REFERENCES

[1] Hwa LG, Lu CL & Liu LC, (2000). Elastic moduli of calcium alumino-silicate glasses studied by Brillouin scattering. *Materials Research Bulletin,* 35, 1285-1292. https://doi.org/10.1016/S0025-5408(00)00317-2.

[2] Cormier L, Ghaleb D, Neuville DR, Delaye JM & Calas G, (2003). Chemical dependence of network topology of calcium aluminosilicate glasses: a computer simulation study. *Journal of Non-Crystalline Solids,* 332, 255-270. https://doi.org/10.1016/j.jnoncrysol.2003.09.012.

[3] Koker ND, (2010). Structure, thermodynamics, and diffusion in $CaAl_2$-Si_2O_8 liquid from first-principles molecular dynamics. *Geochimica et Cosmochimica Acta*, 74, 5657-5671. https://doi.org/10.1016/j.gca.2010.02.024.

[4] Jakse N et al., (2012). Interplay between non-bridging oxygen, triclusters, and fivefold Al coordination in low silica content calcium aluminosilicate melts. *Applied Physics Letters,* 101, 201903. https://doi.org/10.1063/1.4766920.

[5] Stebbins JF, Dubinsky EV, Kanehashi K & Kelsey KE, (2008). Temperature effects on non-bridging oxygen and aluminum coordination number in calcium aluminosilicate glasses and melts. *Geochimica et Cosmochimica Acta,* 72, 910-925. https://doi.org/10.1016/j.gca.2007.11.018.

[6] Cormier L, Neuville DR & Calas G, (2005). Relationship Between Structure and Glass Transition Temperature in Low-silica Calcium Aluminosilicate Glasses: the Origin of the Anomaly at Low Silica Content. *Journal of American Ceramic Society*, 88, 2292-2299. https: //doi.org/10.1111/j.1551-2916.2005.00428.x.

[7] Hennet L et al., (2016). Neutron diffraction of calcium aluminosilicate glasses and melts. *Journal of Non-Crystalline Solids,* 451, 89-93. https: //doi.org/10.1016/j. jnoncrysol.2016.05.018.

[8] Atila A, Ghardia EM, Hasnaouic A & Ouaskit S, (2019). Alumina effect on the structure and properties of calcium aluminosilicate in the percalcic region: A molecular dynamics investigation. *Journal of Non-Crystalline Solids*, 525, 119470. https: //doi.org/10.1016/j.jnoncrysol.2019.119470.

[9] Liu M, Panda S, Suraneni P, & Pestana LR, (2023). Insights from molecular dynamics into the chemistry-structure relationships of calcium aluminosilicate glasses. *Journal of Non-Crystalline Solids* 618, 122545. https://doi.org/ 10.1016/j.jnoncrysol.2023.122545.

[10] Deng L, Du J, (2018). Development of boron oxide potentials for computer simulations of multicomponent oxide glasses. *Journal of American Ceramic Society*, 102(5), 2482-2505. https://doi.org/10.1111/jace.16082.